Making corrections to your proof

Please follow these instructions to mark changes or add notes to your proof. Ensure that you have downloaded the most recent version of Acrobat Reader from **https://get.adobe.com** so you have access to the widest range of annotation tools.

The tools you need to use are contained in **Annotations** in the **Comment** toolbar. You can also right-click on the text for several options. The most useful tools have been highlighted here. If you cannot make the desired change with the tools, please insert a sticky note describing the correction.

Please ensure all changes are visible via the 'Comments List' in the annotated PDF so that your corrections are not missed.

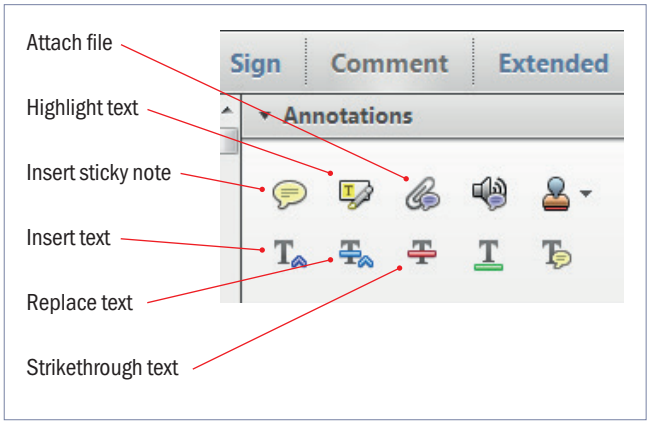

Do not attempt to directly edit the PDF file as changes will not be visible.

Replacing text

To replace text, highlight what you want to change then press the replace text icon, or right-click and press 'Add Note to Replace Text', then insert your text in the pop up box. Highlight the text and right click to style in bold, italic, superscript or subscript.

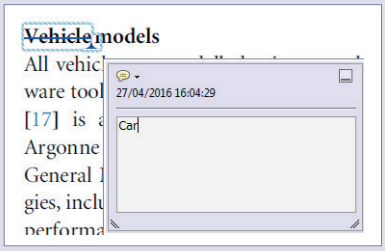

Inserting text

Place your cursor where you want to insert text, then press the insert text icon, or right-click and press 'Insert Text at Cursor', then insert your text in the pop up box. Highlight the text and right click to style in bold, italic, superscript or subscript.

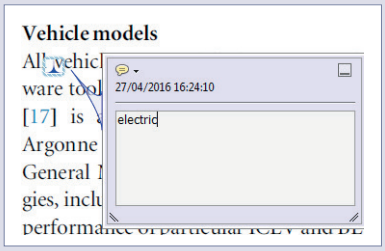

Deleting text

To delete text, highlight what you want to remove then press the strikethrough icon, or right-click and press 'Strikethrough Text'.

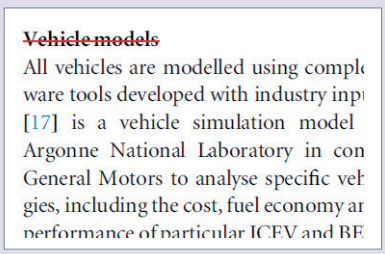

Highlighting text

To highlight text, with the cursor highlight the selected text then press the highlight text icon, or right-click and press 'Highlight text'. If you double click on this highlighted text you can add a comment.

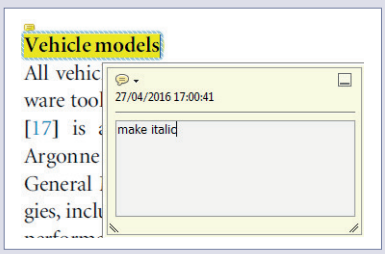

QUERY FORM

JOURNAL: Journal of Physics G: Nuclear and Particle Physics

AUTHOR: V Kumar and P Shukla

TITLE: Charmonia production in p + p collisions under NRQCD formalism

ARTICLE ID: jpgaa7818

The layout of this article has not yet been finalized. Therefore this proof may contain columns that are not fully balanced/matched or overlapping text in inline equations; these issues will be resolved once the final corrections have been incorporated.

Please check that the names of all authors as displayed in the proof are correct, and that all authors are linked correctly to the appropriate affiliations. Please also confirm that the correct corresponding author has been indicated.

If an explicit acknowledgment of funding is required, please ensure that it is indicated in your article. If you already have an Acknowledgments section, please check that the information there is complete and correct.

SQ1
Please be aware that the colour figures in this article will only appear in colour in the online version. If you require colour in the printed journal and have not previously arranged it, please contact the Production Editor now.

Page 1

Q1
Please specify the corresponding author.

Page 15

Q2
Please check the details for any journal references that do not have a link as they may contain some incorrect information. If any journal references do not have a link, please update with correct details and supply a Crossref DOI if available.

Page 16

Q3
Please update the year of publication, volume and page range in references [8, 10].

Q4
Please provide updated details for references [21, 50, 60] if available.

APP Template V1.29 Article id: jpgaa7818 Typesetter: MPS Date received by MPS: 27/06/2017 PE: CE : LE:

UNCORRECTED PROOF

IOP Publishing Journal of Physics G: Nuclear and Particle Physics

J. Phys. G: Nucl. Part. Phys. **00** (2017) 000000 (18pp)

Charmonia production in p + p collisions under NRQCD formalism

Vineet Kumar[1] **and Prashant Shukla**[1,2]

[1] Nuclear Physics Division, Bhabha Atomic Research Center, Mumbai, India
[2] Homi Bhabha National Institute, Anushakti Nagar, Mumbai, India

E-mail: vineet.kumar@cern.ch and pshukla@barc.gov.in

Received 18 October 2016, revised 2 June 2017
Accepted for publication 8 June 2017
Published DD MM 2017

Abstract

Q1 This work presents the differential charmonia production cross sections in high energy p + p collisions calculated using non-relativistic quantum chromodynamics (NRQCD) formalism. The NRQCD formalism, factorizes the quarkonia production cross sections in terms of short distance quantum chromodynamics (QCD) cross sections and long distance matrix elements (LDMEs). The short distance cross sections are calculated in terms of perturbative QCD, and LDMEs are obtained by fitting the experimental data. Measured transverse momentum distributions of χ_c, ψ(2S) and J/ψ in p + $\bar{\text{p}}$ collisions at $\sqrt{s} = 1.8$, 1.96 TeV and in p + p collisions at $\sqrt{s} = 7$, 8 and 13 TeV are used to constrain LDMEs. The feed-down contribution to each state from the higher states are taken into account. The formalism provides a very good description of the data in a wide energy range. The values of LDMEs are used to predict the charmonia cross sections in p + p collisions at 13 and 5 TeV in kinematic bins relevant for the LHC detectors.

Keywords: quarkonia, NRQCD, LHC data

SQ1 (Some figures may appear in colour only in the online journal)

1. Introduction

The quarkonia ($Q\bar{Q}$) have provided useful tools for probing both perturbative and non-perturbative aspects of quantum chromodynamics (QCD) ever since the discovery of J/ψ resonance [1, 2]. The quarkonia states are qualitatively different from most other hadrons since the velocity v of the heavy constituents is small allowing a non-relativistic treatment of bound states. The quarkonia yields are modified in the heavy ion collision due to quark–gluon plasma (QGP) and cold nuclear matter effects which has been demonstrated for J/ψ and Υ in Pb–Pb collisions [3–5]. The ratios of excited to ground state quarkonia yields are considered better probes of QGP since the cold matter effects, which are similar for the ground and

excited states, are expected to cancel in the ratio. At the LHC, the production of charmonium (J/ψ, $\psi(2S)$) and bottomonium ($\Upsilon(1S)$, $\Upsilon(2S)$, $\Upsilon(3S)$) states has been studied in Pb–Pb collisions at $\sqrt{s_{NN}} = 2.76$ TeV and $\sqrt{s_{NN}} = 5.02$ TeV [6–11], affirming the importance of quarkonia measurements in heavy ion collisions. The heavy quarks, due to their high mass ($m_c \sim 1.6\,\mathrm{GeV\,c^{-2}}$, $m_b \sim 4.5\,\mathrm{GeV\,c^{-2}}$), are produced in initial partonic collisions with sufficiently high momentum transfers. Thus, the heavy quark production can be treated perturbatively [12, 13]. The formation of quarkonia out of the two heavy quarks is a non-perturbative process and is treated in terms of different models [14–16]. Most notable models for quarkonia production are the color-singlet model (CSM), the color-evaporation model (CEM), the non-relativistic QCD (NRQCD) factorization approach, and the fragmentation–function approach.

In the CSM [17–20], it is assumed that the $Q\bar{Q}$ pair that evolves into the quarkonium is in a color-singlet (CS) state and has the same spin and angular-momentum as the quarkonium. The production rate of the quarkonium state is related to the absolute values of the CS $Q\bar{Q}$ wave function and its derivatives, evaluated at zero $Q\bar{Q}$ separation. These quantities can be extracted by comparing calculated quarkonium decay rates in the CSM with the experimental measurements. The CSM was successful in predicting quarkonium production rates at relatively low energies [21] but, at high energies, very large corrections appear at next-to-leading order (NLO) and next-to-next-to-leading order (NNLO) in α_s [22–24]. The NRQCD factorization approach comprises the CSM, but also includes color-octet (CO) states. In the CEM [25–27], it is assumed that the produced $Q\bar{Q}$ pair evolves into a quarkonium if its invariant mass is less than the threshold for producing a pair of open-flavor heavy mesons. The nonperturbative probability for the $Q\bar{Q}$ pair to evolve into a quarkonium state is fixed by comparison with the measured production cross section of that quarkonium state. The CEM calculations provide good descriptions of the CDF data for J/ψ, $\psi(2S)$, and χ_c production at $\sqrt{s} = 1.8$ TeV [27] but it fails to predict the quarkonium polarization.

In the NRQCD factorization approach [14], the probability of a $Q\bar{Q}$ pair evolving into a quarkonium is expressed as matrix elements of NRQCD operators in terms of the heavy-quark velocity v in the limit $v \ll 1$. This approach takes into account the complete structure of the $Q\bar{Q}$ Fock space, which is spanned by the state $n = {}^{2S+1}L_J^{[a]}$ with spin S, orbital angular momentum L, total angular momentum J and color multiplicity $a = 1$ (CS), 8 (CO). The $Q\bar{Q}$ pairs, which are produced at short distances in CO states, evolve into physical, CS quarkonia by emitting soft gluons nonperturbatively. In the limit $v \to 0$, the CSM is recovered in the case of S-wave quarkonia. The short distance cross sections can be calculated within the framework of perturbative QCD (pQCD). The long distance matrix elements (LDME), corresponding to the probability of the $Q\bar{Q}$ state to convert to the quarkonium, can be estimated by comparison with the experimental measurements. The leading order (LO) NRQCD gives a good description of J/ψ yields at Tevatron RHIC and LHC energies [28–30]. The NLO corrections to CS J/ψ production have been investigated in [23, 31]. The NLO corrections increase the total CS J/ψ cross section by a factor of two, although at high p_T the corrections can enhance the production by two-three orders of magnitude. [31]. The NLO corrections to J/ψ production via S-wave CO states (${}^1S_0^{[8]}{}^3S_1^{[8]}$) are studied in [32] and the corrections to p_T distributions of both J/ψ yield and polarization are found to be small. In [33], NLO corrections for χ_{cJ} hadroproduction are also studied. Several NLO calculations are performed to obtain the polarization and yield of J/ψ. The J/ψ polarization presents a rather confusing pattern [34–37]. The authors in [35] extracted leading CO LDMEs through a global fit to experimental data of unpolarized J/ψ production in pp, $p\bar{p}$, ep, $\gamma\gamma$ and e^+ e^- collisions. The extracted LDMEs gave an excellent description of the unpolarized J/ψ yields but failed

to reproduce the polarization measured at CDF [38]. In another study [36], it is shown that the measured hadroproduction cross sections and the CDF polarization measurement [38] can be simultaneously described by NRQCD at NLO. The works of [39, 40] and [41] present NLO-NRQCD calculations of J/ψ yields. In both the works, the set of CO LDMEs fitted to p_T distributions measured at HERA and CDF are used to describe the p_T distributions from RHIC and the LHC. The fitted LDMEs of [39] and [41] are incompatible with each other. A recent work [42] gives calculations for both the yields and polarizations of charmonia at the Tevatron and the LHC where the LDMEs are obtained by fitting the Tevatron data only.

Recently, the LHCb measurements of η_c production [43] is investigated from different points of views by several groups using NRQCD formalism [44–46]. Reference [44] considered the η_c measurement as a challenge of NRQCD, while [45] shows that the LHCb measurement results in a very strong constraint on the upper bound of the CO LDME of J/ψ. Reference [46] obtains the CS LDME for η_c by fitting the experimental data to get a good description of η_c production. The prompt double heavy quarkonium production should be a more sensitive testing ground for NRQCD factorization. The experiments at LHC recently published the measurement of double J/ψ production in proton–proton collisions at $\sqrt{s} = 7, 8$ and 13 TeV [47–50]. Full NLO calculations including all CS and CO contributions for this process in the NRQCD framework are not fully established yet. The authors in [51] showed that the LO calculations of the prompt double J/ψ production by NRQCD formalism describes the data only qualitatively. The authors in [52] presented the NLO calculations for the CS channel, which describe the measured LHCb cross section reasonably well, but failed to reproduce the CMS measurements. The complicated situation suggests that further study and a phenomenological test of NRQCD is still an urgent task.

With the LHC has been running for several years, we now have very high quality quarkonia production data in several kinematic regions up to very high transverse momentum which could be used to constrain the LDMEs. In this paper, we use CDF data [53–56] along with new LHC data [57–65] to constrain the LDMEs. The feed-down contribution to each state from the higher states are taken into account. These new LDMEs are then used to predict the J/ψ and $\psi(2S)$ cross-section at 13 TeV and 5 TeV for the kinematical bins relevant to LHC detectors.

The NLO calculations are still evolving and thus we use LO calculations in this work. The values of fitted LDMEs with LO formulations are always useful for straightforward predictions of quarkonia cross section and for the purpose of a comparison with those obtained using NLO formulations. We have given an estimate of uncertainties in the LDMEs due to enhancement of CS J/ψ cross-section by a factor of three expected from NLO corrections.

2. Quarkonia production in p + p collisions

The NRQCD formalism provides a theoretical framework for studying heavy quarkonium production. The dominant processes in the production of heavy mesons ψ are $g + q \to \psi + q$, $q + \bar{q} \to \psi + g$ and $g + g \to \psi + g$. We represent these processes by $a + b \to \psi + X$, where a and b are the light incident partons. The invariant cross-section for the production of a heavy meson ψ can be written in a factorized form as

$$E\frac{\mathrm{d}^3\sigma^{\psi}}{\mathrm{d}^3p} = \sum_{a,b}\int\int \mathrm{d}x_a\,\mathrm{d}x_b\, G_{a/p}(x_a,\,\mu_F^2)\, G_{b/p}(x_b,\,\mu_F^2)\,\frac{\hat{s}}{\pi}\frac{\mathrm{d}\sigma}{\mathrm{d}\hat{t}} \times \delta(\hat{s} + \hat{t} + \hat{u} - M^2), \qquad (1)$$

where $G_{a/p}(G_{b/p})$ is the distribution function (PDF) of the incoming parton $a(b)$ in the incident proton, which depends on the momentum fraction $x_a(x_b)$ and the factorization scale μ_F. The parton level Mandelstam variables $\hat{s}$, $\hat{t}$, and $\hat{u}$ can be expressed in terms of x_a, x_b as

$$\begin{aligned}\hat{s} &= x_a\, x_b\, s\\ \hat{t} &= M^2 - x_a\, \sqrt{s}\, m_T\, \mathrm{e}^{-y}\\ \hat{u} &= M^2 - x_b\, \sqrt{s}\, m_T\, \mathrm{e}^{y},\end{aligned} \tag{2}$$

where $\sqrt{s}$ is the total energy in the centre-of-mass, y is the rapidity and p_T is the transverse momentum of the $Q\bar{Q}$ pair. The mass of the heavy meson is represented by M and m_T is the transverse mass defined as $m_T^2 = p_T^2 + M^2$. Writing down $\hat{s} + \hat{t} + \hat{u} - M^2 = 0$ and solving for x_b, we obtain

$$x_b = \frac{1}{\sqrt{s}} \frac{x_a\, \sqrt{s}\, m_T\, \mathrm{e}^{-y} - M^2}{x_a\, \sqrt{s} - m_T\, \mathrm{e}^{y}}. \tag{3}$$

The double differential cross-section upon p_T and y then is obtained as

$$\frac{\mathrm{d}^2\sigma^{\psi}}{\mathrm{d}p_T\, \mathrm{dy}} = \sum_{a,b} \int_{x_a^{\min}}^{1} \mathrm{d}x_a\, G_{a/A}(x_a, \mu_F^2) G_{b/B}(x_b, \mu_F^2) \times 2p_T \frac{x_a\, x_b}{x_a - \frac{m_T}{\sqrt{s}}\mathrm{e}^{y}} \frac{\mathrm{d}\sigma}{\mathrm{d}\hat{t}}, \tag{4}$$

where the minimum value of x_a is given by

$$x_{a\,\min} = \frac{1}{\sqrt{s}} \frac{\sqrt{s}\, m_T\, \mathrm{e}^{y} - M^2}{\sqrt{s} - m_T\, \mathrm{e}^{-y}}. \tag{5}$$

The parton level cross-section $\mathrm{d}\sigma/\mathrm{d}\hat{t}$ is defined as [14]

$$\frac{\mathrm{d}\sigma}{\mathrm{d}\hat{t}} = \frac{\mathrm{d}\sigma}{\mathrm{d}\hat{t}}(ab \to Q\overline{Q}\,(^{2S+1}L_J) + X)\, M_L(Q\overline{Q}\,(^{2S+1}L_J) \to \psi). \tag{6}$$

The short distance contribution $\mathrm{d}\sigma/\mathrm{d}\hat{t}\,(ab \to Q\overline{Q}\,(^{2S+1}L_J) + X)$, corresponding to the production of a $Q\bar{Q}$ pair in a particular color and spin configuration, can be calculated within the framework of pQCD. The LDME $M_L(Q\overline{Q}\,(^{2S+1}L_J) \to \psi)$ corresponds to the probability the $Q\bar{Q}$ state will convert to the quarkonium wavefunction and can be estimated by comparison with experimental measurements. The short distance invariant differential cross-section is given by

$$\frac{\mathrm{d}\sigma}{\mathrm{d}\hat{t}}(ab \to Q\overline{Q}\,(^{2S+1}L_J) + X) = \frac{|\mathcal{M}|^2}{16\pi\hat{s}^2}, \tag{7}$$

where $|\mathcal{M}|^2$ is the Feynman squared amplitude. We use the expressions for the short distance CS cross-sections given in [66–68] and the CO cross-sections given in [69–71]. The CTEQ6M [72] parametrization is used for parton distribution functions.

The LDMEs scale with a definite power of the relative velocity v of the heavy quarks inside $Q\bar{Q}$ bound states. In the limit $v \ll 1$, the production of quarkonium is based on the $^3S_1^{[1]}$ and $^3P_J^{[1]}$ ($J = 0, 1, 2$) CS states and $^1S_0^{[8]}$, $^3S_1^{[8]}$ and $^3P_J^{[8]}$ CO states. The differential cross section for the direct production of J/ψ can be written as the sum of these contributions,

Table 1. Relevant branching fractions for charmonia [73].

Meson from	to χ_{c0}	to χ_{c1}	to χ_{c2}	to J/ψ
$\psi(2S)$	0.0962	0.092	0.0874	0.595
χ_{c0}				0.0116
χ_{c1}				0.344
χ_{c2}				0.195

$$\begin{aligned}
\mathrm{d}\sigma(J/\psi) = {} & \mathrm{d}\sigma(Q\bar{Q}([^3S_1]_1))M_L(Q\bar{Q}([^3S_1]_1) \to J/\psi) \\
& + \mathrm{d}\sigma(Q\bar{Q}([^1S_0]_8))M_L(Q\bar{Q}([^1S_0]_8) \to J/\psi) \\
& + \mathrm{d}\sigma(Q\bar{Q}([^3S_1]_8))M_L(Q\bar{Q}([^3S_1]_8) \to J/\psi) \\
& + \mathrm{d}\sigma(Q\bar{Q}([^3P_0]_8))M_L(Q\bar{Q}([^3P_0]_8) \to J/\psi) \\
& + \mathrm{d}\sigma(Q\bar{Q}([^3P_1]_8))M_L(Q\bar{Q}([^3P_1]_8) \to J/\psi) \\
& + \mathrm{d}\sigma(Q\bar{Q}([^3P_2]_8))M_L(Q\bar{Q}([^3P_2]_8) \to J/\psi) \\
& + \cdots . \qquad (8)
\end{aligned}$$

The dots represent contribution of terms at higher powers of v. The contributions from the CO matrix elements in equation (8) are suppressed by v^4 compared to the CS matrix elements.

For the case of the p-wave bound states χ_{cJ} (χ_{c0}, χ_{c1} and χ_{c2}), the CS state $Q\bar{Q}[^3P_J]_1$ and the CO state $Q\bar{Q}[^3S_1]_8$ contribute to the same order in v (v^5) because of the angular momentum barrier for the $p-$ wave states, and hence both need to be included. The χ_c differential cross section thus can be written as

$$\begin{aligned}
\mathrm{d}\sigma(\chi_{cJ}) = {} & \mathrm{d}\sigma(Q\bar{Q}([^3P_J]_1))M_L(Q\bar{Q}([^3P_J]_1) \to \chi_{cJ}) \\
& + \mathrm{d}\sigma(Q\bar{Q}([^3S_1]_8))M_L(Q\bar{Q}([^3S_1]_8) \to \chi_{cJ}) \\
& + \cdots . \qquad (9)
\end{aligned}$$

The prompt J/ψ production at LHC energies consists of direct J/ψ production from the initial parton–parton hard scattering and the feed-down contributions to the J/ψ from the decay of heavier charmonium states $\psi(2S)$, χ_{c0}, χ_{c1} and χ_{c2}. The relevant branching fractions are given in table 1 [73]. The prompt $\psi(2S)$ has no significant feed-down contributions from the higher mass states.

The expressions and the values for the CS operators can be found in [69, 70, 74], which are obtained by solving the non-relativistic wavefunctions. The CO operators can not be related to the non-relativistic wavefunctions of $Q\bar{Q}$ since it involves a higher Fock state and thus measured data is used to constrain them. The CS contributions along with their calculated values and CO contributions to be fitted are written below for the prompt J/ψ.

(i) Direct contributions

$$
\begin{aligned}
&M_L(c\bar{c}([^3S_1]_1) \to J/\psi) = 1.2\ \text{GeV}^3\\
&M_L(c\bar{c}([^3S_1]_8) \to J/\psi)\\
&M_L(c\bar{c}([^1S_0]_8) \to J/\psi)\\
&M_L(c\bar{c}([^3P_0]_8) \to J/\psi)\\
&M_L(c\bar{c}([^3P_1]_8) \to J/\psi) = 3\ M_L(c\bar{c}([^3P_0]_8) \to J/\psi)\ [69]\\
&M_L(c\bar{c}([^3P_2]_8) \to J/\psi) = 5\ M_L(c\bar{c}([^3P_0]_8) \to J/\psi)\ [69]
\end{aligned}
\tag{10}
$$

(ii) Feed-down contribution from $\psi(2S)$

$$
\begin{aligned}
&M_L(c\bar{c}([^3S_1]_1) \to \psi(2S)) = 0.76\ \text{GeV}^3\\
&M_L(c\bar{c}([^3S_1]_8) \to \psi(2S))\\
&M_L(c\bar{c}([^1S_0]_8) \to \psi(2S))\\
&M_L(c\bar{c}([^3P_0]_8) \to \psi(2S))\\
&M_L(c\bar{c}([^3P_1]_8) \to \psi(2S)) = 3\ M_L(c\bar{c}([^3P_0]_8) \to \psi(2S))\ [69]\\
&M_L(c\bar{c}([^3P_2]_8) \to \psi(2S)) = 5\ M_L(c\bar{c}([^3P_0]_8) \to \psi(2S))\ [69]
\end{aligned}
\tag{11}
$$

(iii) Feed-down contribution from χ_{cJ}

$$
\begin{aligned}
&M_L(c\bar{c}([^3P_0]_1) \to \chi_{c0}) = 0.054\ m_c^2\ \text{GeV}^5\\
&M_L(c\bar{c}([^3S_1]_8) \to \chi_{c0})
\end{aligned}
\tag{12}
$$

The mass of the charm quark is taken as $m_c = 1.6$ GeV. The short distance cross sections $\mathrm{d}\sigma(Q\bar{Q}([^1S_0]_8))$ and $\mathrm{d}\sigma(Q\bar{Q}([^3P_J]_8))$ have very similar p_T dependence and due to this reason the transverse momentum distribution is sensitive only to a linear combination of their LDMEs. Following the [28, 69] we fit a linear combination

$$
M_L(Q\bar{Q}([^1S_0]_8, [^3P_0]_8) \to \psi) = \frac{M_L(Q\bar{Q}([^1S_0]_8) \to \psi)}{3} + \frac{M_L(Q\bar{Q}([^3P_0]_8) \to \psi)}{m_c^2}
$$

in our calculations.

3. Results and discussions

As discussed in the last section there are two free parameters ($M_L(c\bar{c}([^3S_1]_8 \to J/\psi))$, $M_L(c\bar{c}([^1S_0]_8, [^3P_0]_8) \to J/\psi)$) for J/ψ, two ($M_L(c\bar{c}([^3S_1]_8 \to \psi(2S))$), $M_L(c\bar{c}([^1S_0]_8, [^3P_0]_8) \to \psi(2S))$) for $\psi(2S)$ and one ($M_L(c\bar{c}([^3S_1]_8) \to \chi_{c0})$) for χ_{cJ} to be obtained from the experiments. The measured yields of χ_{cJ} from the following datasets are used to obtain CO matrix elements for χ_{cJ}

(i) CDF results at $\sqrt{S} = 1.8$ TeV [53].
(ii) ATLAS results at $\sqrt{S} = 7$ [61].
(iii) CMS results at $\sqrt{S} = 7$ TeV [59].
(iv) LHCb results at $\sqrt{S} = 7$ TeV [65].

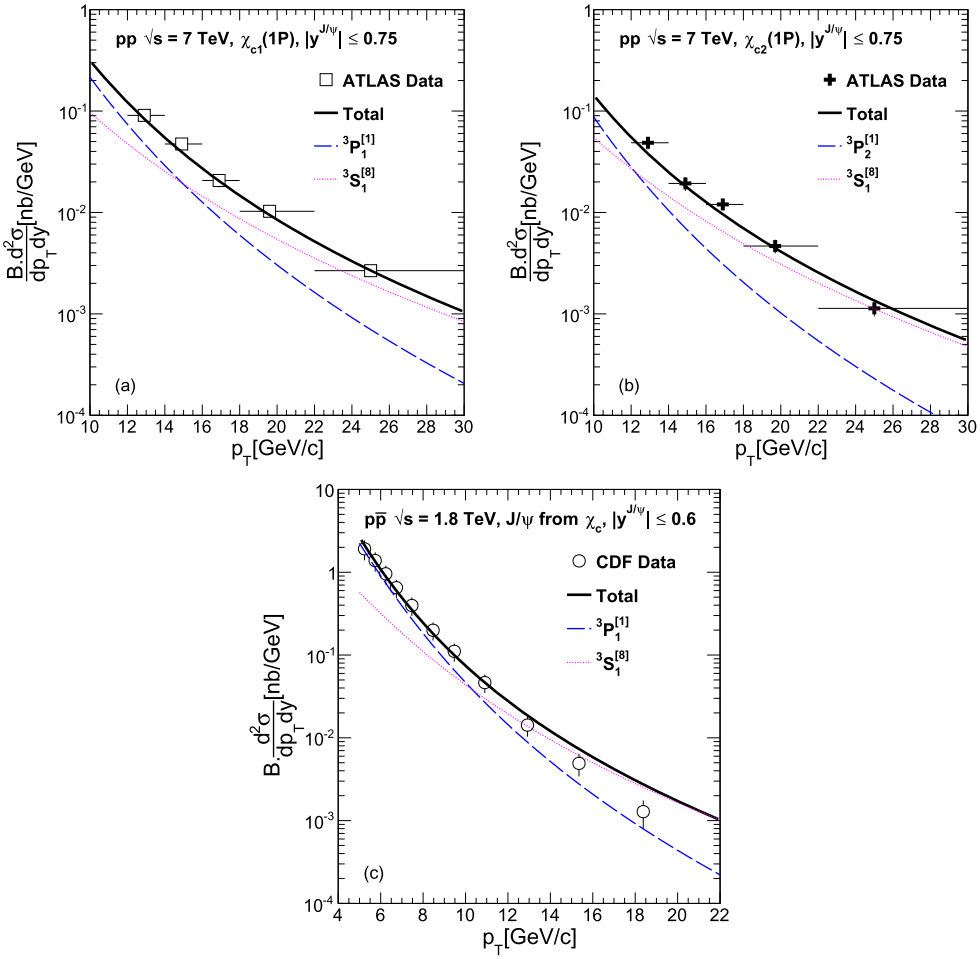

Figure 1. The NRQCD calculations for the production cross section of (a) χ_{c1}, (b) χ_{c2} in p + p collisions at $\sqrt{s} = 7$ TeV and (c) J/ψ from χ_{c1} and χ_{c2} decays in p+$\bar{\text{p}}$ collisions at $\sqrt{s} = 1.8$ TeV as a function of transverse momentum. The calculations are compared with the measured data by the ATLAS experiment at LHC [61] and measured data by the CDF experiment at Tevatron [53]. The χ_c CO LDMEs are obtained by fitting this data.

Figure 1 shows the NRQCD calculations for the production cross sections of (a) χ_{c1}, (b) χ_{c2} in p + p collisions at $\sqrt{s} = 7$ TeV and (c) J/ψ from χ_{c1} and χ_{c2} decays in p+$\bar{\text{p}}$ collisions at $\sqrt{s} = 1.8$ TeV as a function of transverse momentum. The calculations are compared with the measured data by the ATLAS experiment at LHC [61] and measured data by the CDF experiment at Tevatron [53]. The χ_c CO LDMEs are obtained by fitting this data. Figure 2 shows the NRQCD calculations for the production cross section ratios of χ_{c2} and χ_{c1} in p + p collisions at $\sqrt{s} = 7$ TeV as a function of transverse momentum. The calculations are compared with the measured data at LHC in panel (a) CMS data at $\sqrt{s} = 7$ TeV [59] and in panel (b) LHCb data at $\sqrt{s} = 7$ TeV [65]. The χ_c CO LDMEs are obtained by combined fitting of these datasets and its value is

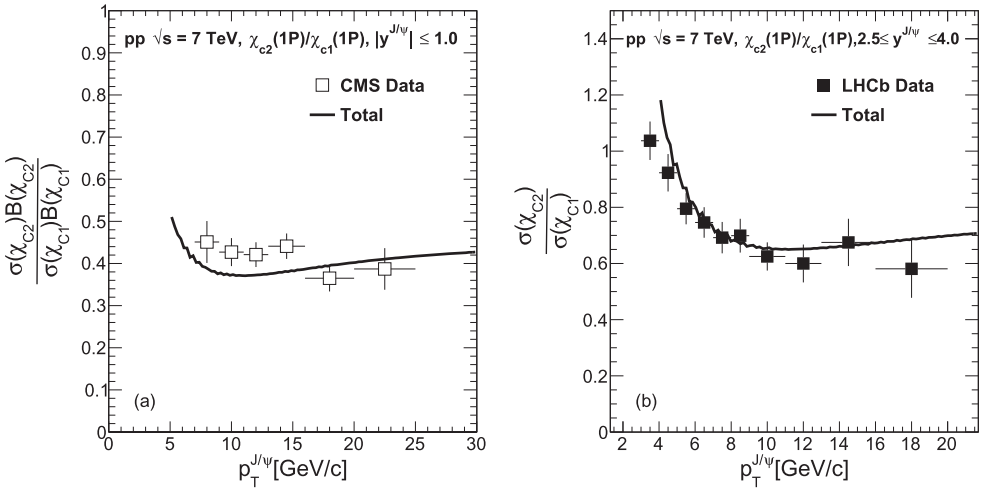

Figure 2. The NRQCD calculations for the production cross section ratios of χ_{c2} and χ_{c1} in p + p collisions at $\sqrt{s} = 7$ TeV as a function of transverse momentum. The calculations are compared with the measured data by the CMS and LHCb experiments at LHC [59, 65]. The χ_c CO LDMEs are obtained by fitting this data.

$$M_L(Q\bar{Q}([^3S_1]_8) \rightarrow \chi_{c0}) = (0.01112 \pm 0.00068)\ \text{GeV}^3, \tag{13}$$

with a combined $\chi^2/\text{d}of = 1.20$.

The measured yields of prompt $\psi(2S)$ from the following datasets are used to obtain CO matrix elements for $\psi(2S)$

(i) CMS results at $\sqrt{S} = 7$ TeV [57, 58].
(ii) ATLAS results at $\sqrt{S} = 7$ and 8 TeV [60].
(iii) CDF results at $\sqrt{S} = 1.8$ TeV [55].
(iv) CDF results at $\sqrt{S} = 1.96$ TeV [56].
(v) LHCb results at $\sqrt{S} = 7$ TeV [62].

Figure 3 shows the NRQCD calculations for the production cross section of ψ(2S) in p + p collisions as a function of transverse momentum compared with the measured data at LHC in panels (a) CMS data at $\sqrt{s} = 7$ TeV [57], (b) CMS data at $\sqrt{s} = 7$ TeV [58], (c) ATLAS data at $\sqrt{s} = 7$ TeV and (d) ATLAS data at $\sqrt{s} = 8$ TeV [60].

Figure 4 shows the NRQCD calculations for the production cross section of ψ(2S) in p+ $\bar{\text{p}}$ and p + p collisions as a function of transverse momentum compared with the measured data in panels (a) CDF data at $\sqrt{s} = 1.8$ TeV [55], (b) CDF data at $\sqrt{s} = 1.96$ TeV [56] and (c) LHCb data at $\sqrt{s} = 7$ TeV [62]. The LDMEs are obtained by a combined fit of the Tevatron and LHC data

We obtain following values of $\psi(2S)$ CO matrix elements by a combined fit of the Tevatron and LHC data

$$\begin{aligned} M_L(c\bar{c}([^3S_1]_8) \rightarrow \psi(2S)) &= (0.00362 \pm 0.00006 \pm 0.00002)\ \text{GeV}^3 \\ M_L(Q\bar{Q}([^1S_0]_8, [^3P_0]_8) \rightarrow \psi(2S)) &= (0.02280 \pm 0.00028 \pm 0.00034)\ \text{GeV}^3 \end{aligned} \tag{14}$$

with a $\chi^2/\text{d}of = 2.54$.

Here the first error is due to the fitting and the second error is obtained by enhancing the CS cross section three times. It is due to the fact that NLO corrections enhance the total CS J/

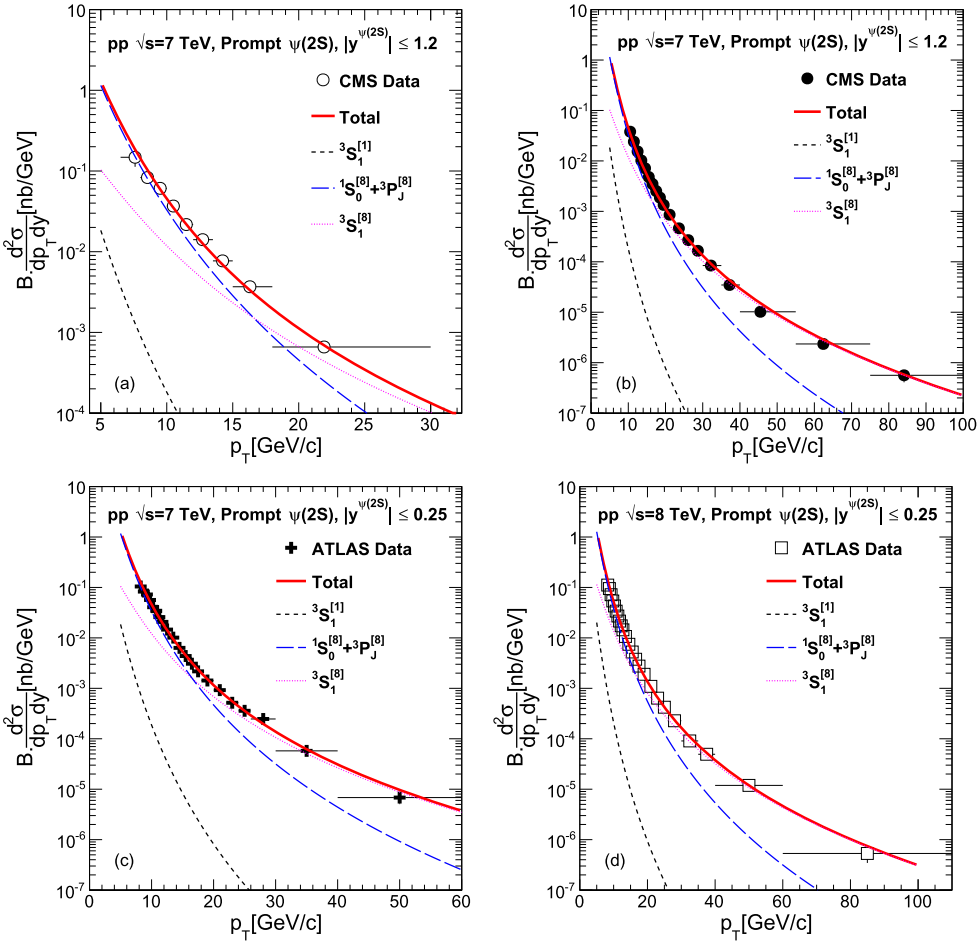

Figure 3. The NRQCD calculations for the production cross section of ψ(2S) in p + p collisions as a function of transverse momentum compared with the measured data at LHC (a) CMS data at $\sqrt{s} = 7$ TeV [57] (b) CMS data at $\sqrt{s} = 7$ TeV [58] (c) ATLAS data at $\sqrt{s} = 7$ TeV and (d) ATLAS data at $\sqrt{s} = 8$ TeV [60]. The LDMEs are obtained by a combined fit of the LHC and Tevatron data.

ψ production by a factor of 2 [31]. The NLO corrections to J/ψ production via S-wave CO states ($^1S_0^{[8]}{}^3S_1^{[8]}$) are found to be small [32].

To fit the remaining two parameters of J/ψ we use the combined fit for the following datasets of prompt J/ψ yields

(i) CMS results at $\sqrt{S} = 7$ TeV [57, 58].
(ii) ATLAS results at $\sqrt{S} = 7$ and 8 TeV [60].
(iii) CDF results at $\sqrt{S} = 1.8$ TeV [55].
(iv) CDF results at $\sqrt{S} = 1.96$ TeV [56].
(v) LHCb results at $\sqrt{S} = 7$ TeV [63].
(vi) LHCb results at $\sqrt{S} = 13$ TeV [64].

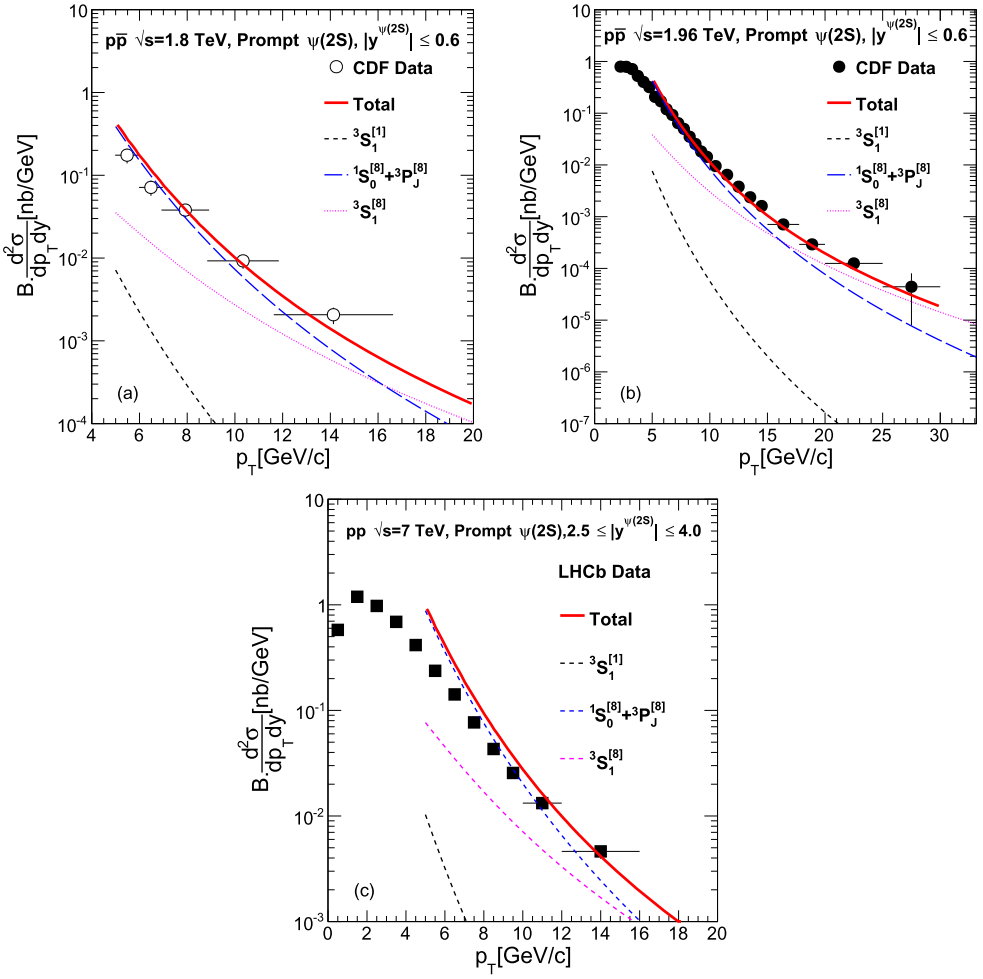

Figure 4. The NRQCD calculations for the production cross section of ψ(2S) in p+$\bar{\text{p}}$ and p + p collisions as a function of transverse momentum compared with the measured data (a) CDF data at $\sqrt{s} = 1.8$ TeV [55], (b) CDF data at $\sqrt{s} = 1.96$ TeV [56] and (c) LHCb data at $\sqrt{s} = 7$ TeV [62]. The LDMEs are obtained by a combined fit of the Tevatron and LHC data.

Figure 5 shows the NRQCD calculations for production cross section of J/ψ in p + p collisions as a function of transverse momentum compared with the measured data at LHC in panels (a) CMS data at $\sqrt{s} = 7$ TeV [57] and (b) CMS data at $\sqrt{s} = 7$ TeV [58] (c) ATLAS data at $\sqrt{s} = 7$ TeV and (d) ATLAS data at $\sqrt{s} = 8$ TeV [60]. Figure 6 shows the NRQCD calculations for the production cross section of J/ψ in p+$\bar{\text{p}}$ collisions as compared with the measured data at Tevatron in panels (a) CDF data at $\sqrt{s} = 1.8$ TeV [55] and (b) CDF data at $\sqrt{s} = 1.96$ TeV [56]. Figure 7 shows the the NRQCD calculations of production cross section of J/ψ in p + p collisions compared with the forward rapidity data measured at LHC in panels (a) LHCb data at $\sqrt{s} = 7$ TeV [63] and (b) LHCb data at $\sqrt{s} = 13$ TeV [64]. We obtain following values of J/ψ CO matrix elements by a combined fit of the Tevatron and the LHC data

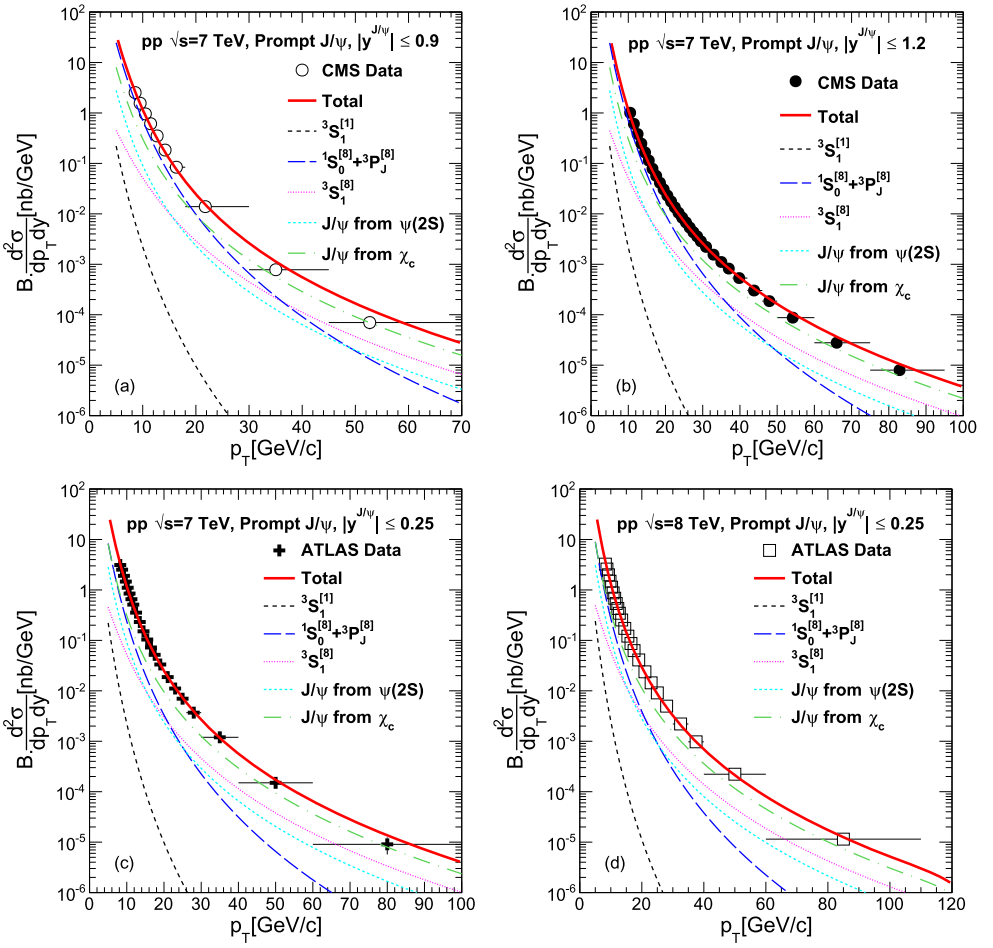

Figure 5. The NRQCD calculations for the production cross section of J/ψ in p + p collisions as a function of transverse momentum compared with the measured data at LHC (a) CMS data at $\sqrt{s} = 7$ TeV [57] (b) CMS data at $\sqrt{s} = 7$ TeV [58] (c) ATLAS data at $\sqrt{s} = 7$ TeV and (d) ATLAS data at $\sqrt{s} = 8$ TeV [60]. The LDMEs are obtained by a combined fit of the LHC and Tevatron data.

$$M_L(c\bar{c}([^3S_1]_8) \rightarrow J/\psi) = (0.00206 \pm 0.00014 \pm 0.00001)\ \text{GeV}^3$$
$$M_L(Q\bar{Q}([^1S_0]_8, [^3P_0]_8) \rightarrow J/\psi) = (0.06384 \pm 0.00106 \pm 0.00062)\ \text{GeV}^3 \quad (15)$$

with a $\chi^2/\text{d}of = 2.76$.

Table 2 shows χ_{c0} LDMEs extracted in present analysis along with the results from other analysis. The value of charm quark mass as well as the PDFs used in the calculations are also shown in the table. The short distance calculations are at LO except the last row in the table. We have made a major extension in fitting the χ_c LDME. All the earlier calculations [29, 30, 69] use only CDF data to fit the χ_c LDME. We use CDF data [53] along with the data from LHC [59, 61, 65] to constrain the CO LDME of χ_c. The new high energy LHC data require larger value of $(M_L(c\bar{c}([^3S_1]_8) \rightarrow \chi_{c0}))$ to fit the data.

Table 3 shows $\psi(2S)$ LDMEs extracted in the present analysis along with the results from other works. All the calculations are at LO in α_s. The calculations in [28, 29, 69] use only

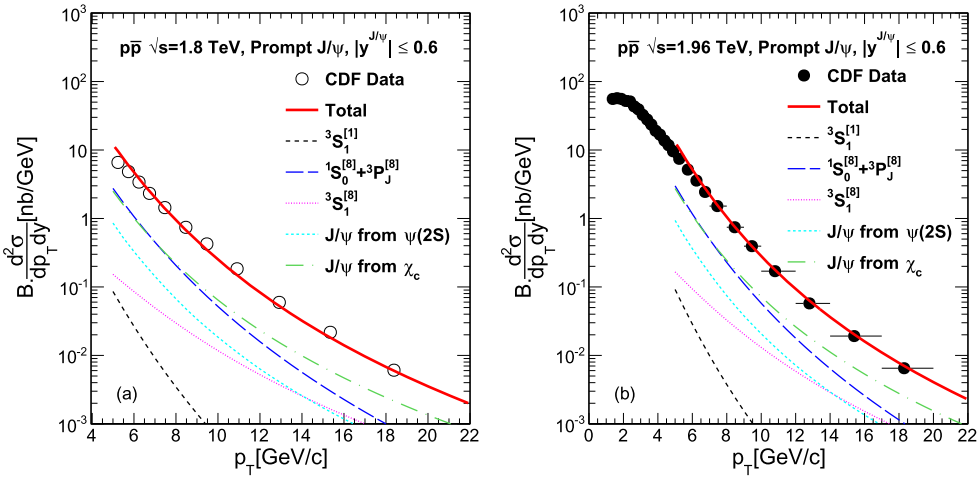

Figure 6. The NRQCD calculations for the production cross section of J/ψ in p+$\bar{\text{p}}$ collisions as a function of transverse momentum compared with the measured data at Tevatron (a) CDF data at $\sqrt{s} = 1.8$ TeV [55] and (b) CDF data at $\sqrt{s} = 1.96$ TeV [56]. The LDMEs are obtained by a combined fit of the LHC and Tevatron data.

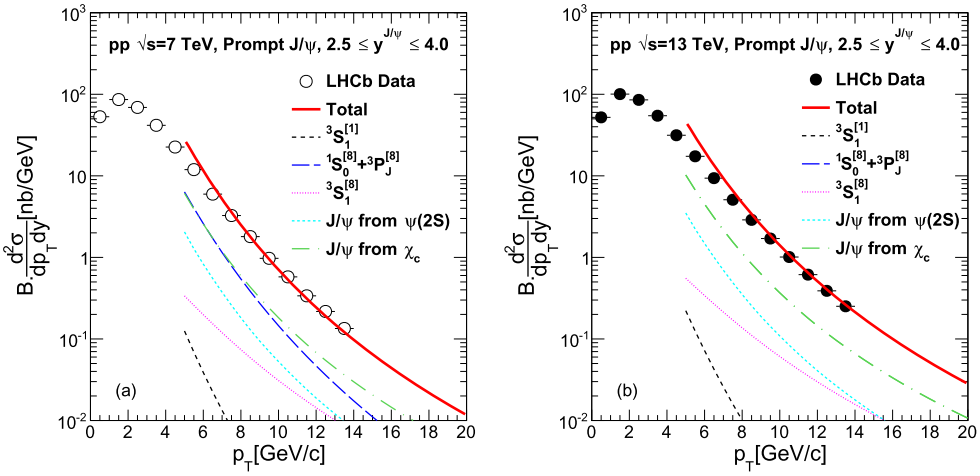

Figure 7. The NRQCD calculations for the production cross section of J/ψ in p + p collisions as a function of transverse momentum compared with the measured data at LHC (a) LHCb data at $\sqrt{s} = 7$ TeV [63] and (b) LHCb data at $\sqrt{s} = 13$ TeV [64]. The LDMEs are obtained by a combined fit of the LHC and Tevatron data.

CDF data to fit the LDMEs while [30] use CDF and LHC data at mid-rapidity. In our analysis we use data from CDF [55, 56] and LHC data in mid rapidity [57, 58, 60] as well as LHC data in forward rapidity [62], both the datasets covering a much wider p_T range. Our value of matrix element $M_L(c\bar{c}([^3S_1]_8 \rightarrow \psi(2S))$ is similar with other analysis. The value of linear-combination, $M_L(c\bar{c}([^1S_0]_8, [^3P_0]_8) \rightarrow \psi(2S))$, varies significantly from 0.0022 to 0.01246 between different analysis. As it can be seen from table 3, the high energy LHC data require larger value of $M_L(c\bar{c}([^1S_0]_8, [^3P_0]_8) \rightarrow \psi(2S))$.

Table 2. Comparison of χ_{c0} LDMEs. The short distance calculations are at LO except [75](NLO).

Reference	PDF	m_c (GeV)	$M_L(c\bar{c}([^3P_0]_1) \to \chi_{c0})$ (GeV^5)	$M_L(c\bar{c}([^3S_1]_8) \to \chi_{c0})$ (GeV^3)
ours	CTEQ6M	1.6	$0.054m_c^2$	0.01112 ± 0.00068
[69]	MRSD0	1.48	—	0.0098 ± 0.0013
[29]	MRST98LO	1.5	0.089 ± 0.013	0.0023 ± 0.0003
[29]	CTEQ5L	1.5	0.091 ± 0.013	0.0019 ± 0.0002
[30]	MSTW08LO	1.4	$0.054m_c^2$	0.00187 ± 0.00025
[75](LO)	CTEQ6L	1.5	—	0.00031 ± 0.00009
[75](NLO)	CTEQ6M	1.5	—	0.0021 ± 0.00004

Table 3. Comparison of ψ(2S) LDMEs. The short distance calculations are at LO.

Reference	PDF	m_c (GeV)	$M_L(c\bar{c}([^3S_1]_1 \to \psi(2S)))$ (GeV^3)	$M_L(c\bar{c}([^3S_1]_8 \to \psi(2S)))$ (GeV^3)	$M_L(c\bar{c}([^1S_0]_8, [^3P_0]_8) \to \psi(2S))$ (GeV^3)
ours	CTEQ6M	1.6	0.76	0.00362 ± 0.00006	0.02280 ± 0.00028
[69]	MRSD0	1.48	—	0.0046 ± 0.0010	0.0059 ± 0.0019
[29]	MRST98LO	1.5	0.65 ± 0.6	0.0042 ± 0.0010	0.0037 ± 0.0014
[29]	CTEQ5L	1.5	0.67 ± 0.7	0.0037 ± 0.0090	0.0022 ± 0.001
[30]	MSTW08LO	1.4	0.76	0.0033 ± 0.00021	0.01067 ± 0.0009
[28]	CTEQ4L	1.5	—	0.0044 ± 0.0008	0.00514 ± 0.0016
[28]	GRV94LO	1.5	—	0.0046 ± 0.0008	0.00457 ± 0.0014
[28]	MRSR2	1.5	—	0.0056 ± 0.0011	0.01246 ± 0.0027

Table 4. Comparison of J/ψ LDMEs. The short distance calculations are at LO except [39].

Reference	PDF	m_c (GeV)	$M_L(c\bar{c}([^3S_1]_1 \to J/\psi))$ (GeV^3)	$M_L(c\bar{c}([^3S_1]_8 \to J/\psi))$ (GeV^3)	$M_L(c\bar{c}([^1S_0]_8, [^3P_0]_8) \to J/\psi))$ (GeV^3)
ours	CTEQ6M	1.6	1.2	0.00206 ± 0.00014	0.06384 ± 0.00106
[69]	MRSD0	1.48	—	0.0066 ± 0.0021	0.0220 ± 0.050
[29]	MRST98LO	1.5	1.3 ± 0.1	0.0044 ± 0.0007	0.026 ± 0.0026
[29]	CTEQ5L	1.5	1.4 ± 0.1	0.0039 ± 0.0007	0.0194 ± 0.0021
[30]	MSTW08LO	1.4	1.2	0.0013 ± 0.0013	0.0239 ± 0.0115
[28]	CTEQ4L	1.5	—	0.0106 ± 0.0014	0.0125 ± 0.0032
[28]	GRV94LO	1.5	—	0.0112 ± 0.0014	0.0114 ± 0.0032
[28]	MRSR2	1.5	—	0.0140 ± 0.0022	0.0311 ± 0.0059
[39]	CTEQ6M	1.5	1.32	0.00312 ± 0.00093	0.00962 ± 0.0008

Table 4 shows J/ψ LDMEs extracted in present analysis along with the results from other works. All the calculations except [39] are at LO in α_s. The calculations in [28, 29, 69] use only CDF data to fit the LDMEs while [30] uses CDF, RHIC and LHC data at mid-rapidity. In our analysis, we use data from CDF [55, 56] and LHC data in mid rapidity [57, 58, 60] as well as LHC data in forward rapidity [63, 64], both the datasets covering a much wider p_T

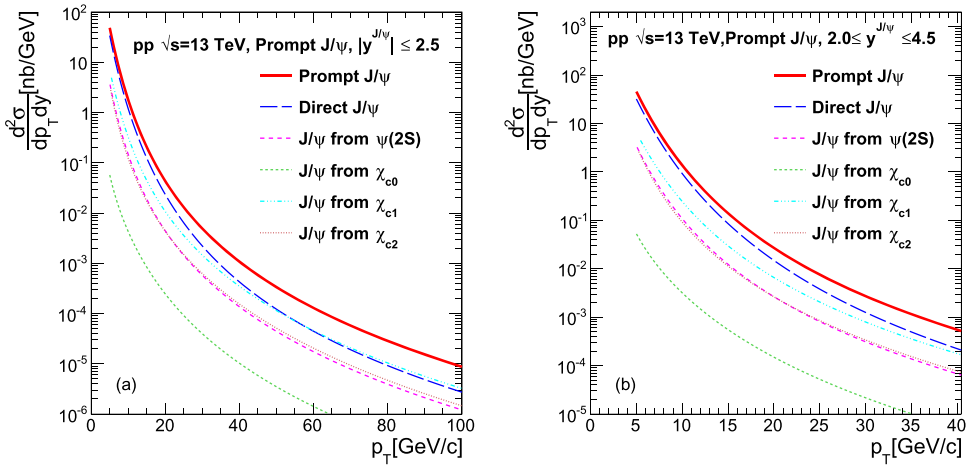

Figure 8. The NRQCD calculations for the production cross section of J/ψ in p + p collisions as a function of transverse momentum at $\sqrt{s} = 13$ TeV. The calculations are shown in the kinematic bins relevant to (a) CMS, ATLAS and (b) ALICE, LHCb detectors at LHC. For the J/ψ meson all the relevant contributions from higher mass states are also shown.

range. The value of the matrix element $M_L(c\bar{c}([^3S_1]_8 \rightarrow J/\psi))$ is different in different analysis. The large error present in $M_L(c\bar{c}([^3S_1]_8 \rightarrow J/\psi))$ in [30] is significantly improved by our simultaneous fitting of several datasets. The value of linear-combination, $M_L(c\bar{c}([^1S_0]_8, [^3P_0]_8) \rightarrow J/\psi)$, varies significantly from 0.0114 to 0.06384 (our value) between different analysis at LO. The NLO analysis [39] does not fit the linear combination but fit both $M_L(c\bar{c}([^1S_0]_8 \rightarrow J/\psi))$ and $M_L(c\bar{c}([^3P_0]_8 \rightarrow J/\psi)))$ LDMEs independently and their values are given as 0.0450 ± 0.0072 and -0.0121 ± 0.0035, respectively . The value of $M_L(c\bar{c}([^1S_0]_8, [^3P_0]_8) \rightarrow J/\psi)$ is very small for [39] because of the negative value of $M_L(c\bar{c}([^3P_0]_8 \rightarrow J/\psi))$.

We use our newly constrained CO LDMEs shown in equation (15) to predict the J/ψ cross-section at 13 TeV and 5 TeV for the kinematical bins relevant to LHC detectors. Figure 8 shows the NRQCD calculations of production cross section of J/ψ in p + p collisions as a function of transverse momentum at $\sqrt{s} = 13$ TeV. Figure 9 is the same as figure 8 but at $\sqrt{s} = 5$ TeV. Both the figures give calculations in the kinematic bins relevant for (a) CMS, ATLAS and (b) ALICE, LHCb detectors at LHC. For the J/ψ meson all the relevant contributions from higher mass states are also shown.

4. Summary

We have presented NRQCD calculations for the differential production cross sections of prompt J/ψ and prompt ψ(2S) in p + p collisions. For the J/ψ meson, all the relevant contributions from higher mass states are estimated. Measured transverse momentum distributions of ψ(2S), χ_c and J/ψ in p +$\bar{\text{p}}$ collisions at $\sqrt{s} = 1.8$, 1.96 TeV and in p + p collisions at 7, 8 and 13 TeV are used to constrain LDMEs. The calculations for prompt J/ψ and prompt ψ(2S) are compared with the measured data at Tevatron and LHC. The formalism provides very good description of the data in wide energy range. The values of LDMEs are used to predict the charmonia cross sections in p + p collisions at 13 and 5 TeV in kinematic

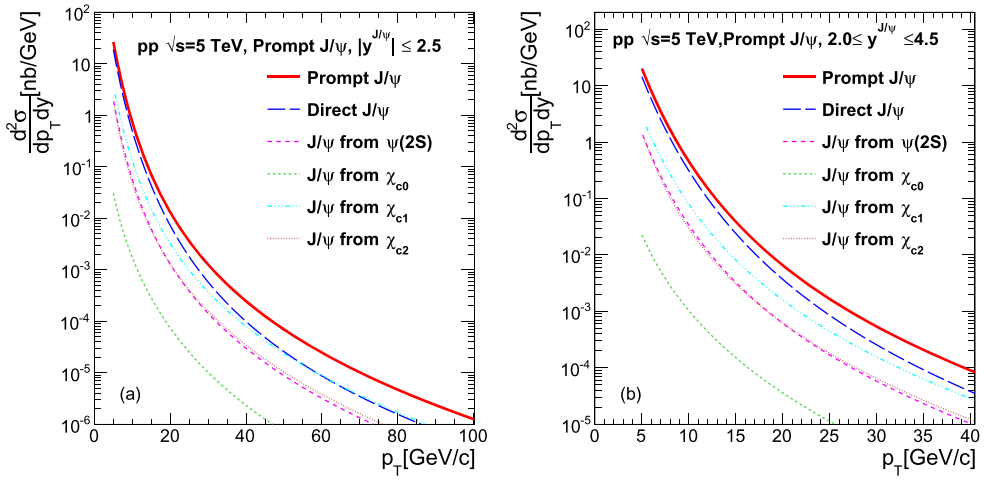

Figure 9. The NRQCD calculations for the production cross section of J/ψ in p + p collisions as a function of transverse momentum at $\sqrt{s} = 5$ TeV. The calculations are shown in the kinematic bins relevant to (a) CMS, ATLAS and (b) ALICE, LHCb detectors at LHC. For the J/ψ meson all the relevant contributions from higher mass states are also shown.

bins relevant for LHC detectors. We compare the LDMEs for charmonia obtained in this analysis with the results from earlier works. At high p_T, the CS contribution is very small and thus the LHC data in large p_T range help to constrain the relative contributions of different colour octet contributions. The high energy LHC data require a smaller value of the LDME $M_L(c\bar{c}([^3S_1]_8 \rightarrow \psi))$ and a larger value for the combination $M_L(c\bar{c}([^1S_0]_8, [^3P_0]_8) \rightarrow \psi)$ of LDMEs. In summary, we present a comprehensive lowest-order analysis of hadroproduction data, including very recent LHC data. The values of fitted LDMEs will be useful for predictions of quarkonia cross sections and for the purpose of a comparison with those obtained using NLO formulations.

Acknowledgments

We acknowledge the fruitful discussions on this topic with Rishi Sharma.

References

[1] Augustin J E *et al* (SLAC-SP-017 Collaboration) 1974 Discovery of a narrow resonance in e+ e− annihilation *Phys. Rev. Lett.* **33** 1406
Augustin J E *et al* (SLAC-SP-017 Collaboration) 1976 Discovery of a narrow resonance in e+ e− annihilation *Adv. Exp. Phys.* **5** 141
[2] Aubert J J *et al* (E598 Collaboration) 1974 Experimental observation of a heavy particle *J. Phys. Rev. Lett.* **33** 1404
[3] Braun-Munzinger P, Koch V, Schäfer T and Stachel J 2016 Properties of hot and dense matter from relativistic heavy ion collisions *Phys. Rept.* **621** 76
[4] Kumar V, Shukla P and Vogt R 2015 Quarkonia suppression in PbPb collisions at $\sqrt{s_{NN}} = 2.76$ TeV *Phys. Rev.* C **92** 024908
[5] Mocsy A, Petreczky P and Strickland M 2013 Quarkonia in the quark gluon plasma *Int. J. Mod. Phys.* A **28** 1340012

[6] Chatrchyan S *et al* (CMS Collaboration) 2012 Observation of sequential Upsilon suppression in PbPb collisions *Phys. Rev. Lett.* **109** 222301
[7] Khachatryan V *et al* (CMS Collaboration) 2014 Measurement of Prompt $\psi(2S) \rightarrow J/\psi$ Yield Ratios in Pb–Pb and $p-p$ Collisions at $\sqrt{s_{NN}} = 2.76$ TeV *Phys. Rev. Lett.* **113** 262301
[8] Khachatryan V *et al* (CMS Collaboration) Suppression and azimuthal anisotropy of prompt and nonprompt J/ψ production in PbPb collisions at $\sqrt{s_{NN}} = 2.76$ TeV *Eur. Phys. J.* C arXiv:1610.00613
[9] Sirunyan A M *et al* (CMS Collaboration) 2017 Relative modification of prompt ψ(2S) and J/ψ yields from pp to PbPb collisions at $\sqrt{s_{\rm NN}} = 5.02$ TeV *Phys. Rev. Lett.* **118** 162301
[10] Khachatryan V *et al* (CMS Collaboration) Suppression of $\Upsilon(1S)$, $\Upsilon(2S)$ and $\Upsilon(3S)$ production in PbPb collisions at $\sqrt{s_{NN}} = 2.76$ TeV *Phys. Lett.* B arXiv:1611.01510
[11] Abelev B B *et al* (ALICE Collaboration) 2014 Centrality, rapidity and transverse momentum dependence of J/ψ suppression in Pb–Pb collisions at $\sqrt{s_{NN}} = 2.76$ TeV *Phys. Lett.* B **734** 314
[12] Nason P, Dawson S and Ellis R K 1988 The total cross-section for the production of heavy quarks in hadronic collisions *Nucl. Phys.* B **303** 607
[13] Nason P, Dawson S and Ellis R K 1989 The one particle inclusive differential cross-section for heavy quark production in hadronic collisions *Nucl. Phys.* B **327** 49
Nason P, Dawson S and Ellis R K 1990 The one particle inclusive differential cross-section for heavy quark production in hadronic collisions *Nucl. Phys.* B **335** 260
[14] Bodwin G T, Braaten E and Lepage G P 1995 Rigorous QCD analysis of inclusive annihilation and production of heavy quarkonium *Phys. Rev.* D **51** 1125
Bodwin G T, Braaten E and Lepage G P 1997 Rigorous QCD analysis of inclusive annihilation and production of heavy quarkonium *Phys. Rev.* D **55** 5853
[15] Brambilla N *et al* 2011 Heavy quarkonium: progress, puzzles, and opportunities *Eur. Phys. J.* C **71** 1534
[16] Brambilla N *et al* 2014 QCD and strongly coupled gauge theories: challenges and perspectives *Eur. Phys. J.* C **74** 2981
[17] Einhorn M B and Ellis S D 1975 Hadronic production of the new resonances: probing gluon distributions *Phys. Rev.* D **12** 2007
[18] Ellis S D, Einhorn M B and Quigg C 1976 Comment on hadronic production of psions *Phys. Rev. Lett.* **36** 1263
[19] Carlson C E and Suaya R 1976 Hadronic production of J/ψ mesons *Phys. Rev.* D **14** 3115
[20] Berger E L and Jones D L 1981 Inelastic photoproduction of J/ψ and Υ by gluons *Phys. Rev.* D **23** 1521
[21] Schuler G A Quarkonium production and decays arXiv:hep-ph/9403387
[22] Artoisenet P, Lansberg J P and Maltoni F 2007 Hadroproduction of J/ψ and υ in association with a heavy-quark pair *Phys. Lett.* B **653** 60
[23] Campbell J M, Maltoni F and Tramontano F 2007 QCD corrections to J/ψ and Υ production at hadron colliders *Phys. Rev. Lett.* **98** 252002
[24] Artoisenet P, Campbell J M, Lansberg J P, Maltoni F and Tramontano F 2008 Υ production at fermilab tevatron and LHC energies *Phys. Rev. Lett.* **101** 152001
[25] Fritzsch H 1977 Producing heavy quark flavors in hadronic collisions: a test of quantum chromodynamics *Phys. Lett.* B **67** 217
[26] Amundson J F, Eboli O J P, Gregores E M and Halzen F 1996 Colorless states in perturbative QCD: charmonium and rapidity gaps *Phys. Lett.* B **372** 127
[27] Amundson J F, Eboli O J P, Gregores E M and Halzen F 1997 Quantitative tests of color evaporation: charmonium production *Phys. Lett.* B **390** 323
[28] Beneke M and Kramer M 1997 1, Direct J/ψ and ψ' polarization and cross-sections at the Tevatron *Phys. Rev.* D **55** 5269
[29] Braaten E, Kniehl B A and Lee J 2000 Polarization of prompt J/ψ at the tevatron *Phys. Rev.* D **62** 094005
[30] Sharma R and Vitev I 2013 High transverse momentum quarkonium production and dissociation in heavy ion collisions *Phys. Rev.* C **87** 044905
[31] Gong B and Wang J X 2008 Next-to-leading-order QCD corrections to J/ψ polarization at Tevatron and Large Hadron Collider energies *Phys. Rev. Lett.* **100** 232001
[32] Gong B, Li X Q and Wang J X 2009 QCD corrections to J/ψ production via color octet states at tevatron and LHC *Phys. Lett.* B **673** 197

Gong B, Li X Q and Wang J X 2010 QCD corrections to J/ψ production via color octet states at tevatron and LHC *Phys. Lett.* **693** 612
[33] Ma Y Q, Wang K and Chao K T 2011 QCD radiative corrections to χ_{cJ} production at hadron colliders *Phys. Rev.* D **83** 111503
[34] Butenschoen M and Kniehl B A 2012 J/ψ polarization at tevatron and LHC: nonrelativistic-QCD factorization at the crossroads *Phys. Rev. Lett.* **108** 172002
[35] Butenschoen M and Kniehl B A 2013 Next-to-leading-order tests of NRQCD factorization with J/ψ yield and polarization *Mod. Phys. Lett.* A **28** 1350027
[36] Chao K T, Ma Y Q, Shao H S, Wang K and Zhang Y J 2012 J/ψ Polarization at hadron colliders in nonrelativistic QCD *Phys. Rev. Lett.* **108** 242004
[37] Gong B, Wan L P, Wang J X and Zhang H F 2013 Polarization for prompt J/ψ and ψ(2S) production at the tevatron and LHC *Phys. Rev. Lett.* **110** 042002
[38] Abulencia A *et al* (CDF Collaboration) 2007 Polarization of J/ψ and ψ_{2S} mesons produced in $p\bar{p}$ collisions at $\sqrt{s} = 1.96$-TeV *Phys. Rev. Lett.* **99** 132001
[39] Butenschoen M and Kniehl B A 2011 Reconciling J/ψ production at HERA, RHIC, Tevatron, and LHC with NRQCD factorization at next-to-leading order *Phys. Rev. Lett.* **106** 022003
[40] Butenschoen M and Kniehl B A 2011 World data of J/ψ production consolidate NRQCD factorization at NLO *Phys. Rev.* D **84** 051501
[41] Ma Y Q, Wang K and Chao K T 2011 J/$\psi(\psi')$ production at the tevatron and LHC at $\mathcal{O}(\alpha_s^4 v^4)$ in nonrelativistic QCD *Phys. Rev. Lett.* **106** 042002
[42] Shao H S, Han H, Ma Y Q, Meng C, Zhang Y J and Chao K T 2015 Yields and polarizations of prompt J/ψ and $\psi(2S)$ production in hadronic collisions *J. High Energy Phys.* JHEP05 (2015)103
[43] Aaij R *et al* (LHCb Collaboration) 2015 Measurement of the $\eta_c(1S)$ production cross-section in proton-proton collisions via the decay $\eta_c(1S) \to p\bar{p}$ *Eur. Phys. J.* C **75** 311
[44] Butenschoen M, He Z G and Kniehl B A 2015 η_c production at the LHC challenges nonrelativistic-QCD factorization *Phys. Rev. Lett.* **114** 092004
[45] Han H, Ma Y Q, Meng C, Shao H S and Chao K T 2015 η_c production at LHC and indications on the understanding of J/ψ production *Phys. Rev. Lett.* **114** 092005
[46] Zhang H F, Sun Z, Sang W L and Li R 2015 Impact of η_c hadroproduction data on charmonium production and polarization within NRQCD framework *Phys. Rev. Lett.* **114** 092006
[47] Aaij R *et al* (LHCb Collaboration) 2012 Observation of J/ψ pair production in pp collisions at $\sqrt{s} = 7$ TeV *Phys. Lett.* B **707** 52
[48] Khachatryan V *et al* (CMS Collaboration) 2014 Measurement of prompt J/ψ pair production in pp collisions at $\sqrt{s} = 7$ Tev *J. High Energy Phys.* **1409** JHEP09(2014)094
[49] Aaboud M *et al* (ATLAS Collaboration) 2017 Measurement of the prompt J/ψ pair production cross-section in pp collisions at $\sqrt{s} = 8$TeV with the ATLAS detector *Eur. Phys. J.* C **77** 76
[50] Aaij R *et al* (LHCb Collaboration) Measurement of the J/ψ pair production cross-section in pp collisions at $\sqrt{s} = 13$ TeV arXiv:1612.07451.
[51] He Z G and Kniehl B A 2015 Complete nonrelativistic-QCD prediction for prompt double J/ψ hadroproduction *Phys. Rev. Lett.* **115** 022002
[52] Sun L P, Han H and Chao K T 2016 Impact of J/ψ pair production at the LHC and predictions in nonrelativistic QCD *Phys. Rev.* D **94** 074033
[53] Abe F *et al* (CDF Collaboration) 1997 Production of J/ψ mesons from χ_c meson decays in $p\bar{p}$ collisions at $\sqrt{s} = 1.8$ TeV *Phys. Rev. Lett.* **79** 578
[54] Abulencia A *et al* (CDF Collaboration) 2007 Measurement of $\sigma_{\chi_{c2}}\mathcal{B}(\chi_{c2} \to J/\psi\gamma)/\sigma_{\chi_{c1}}\mathcal{B}(\chi_{c1} \to J/\psi\gamma)$ in $p\bar{p}$ collisions at $\sqrt{s} = 1.96$-TeV. *Phys. Rev. Lett.* **98** 232001
[55] Abe F *et al* (CDF Collaboration) 1997 J/ψ and $\psi(2S)$ production in $p\bar{p}$ collisions at $\sqrt{s} = 1.8$ TeV *Phys. Rev. Lett.* **79** 572
[56] Acosta D *et al* (CDF Collaboration) 2005 Measurement of the J/ψ meson and $b-$ hadron production cross sections in $p\bar{p}$ collisions at $\sqrt{s} = 1960$ GeV *Phys. Rev.* D **71** 032001
[57] Chatrchyan S *et al* (CMS Collaboration) 2012 J/ψ and ψ_{2S} production in pp collisions at $\sqrt{s} = 7$ *TeV J. High Energy Phys.* JHEP02(2012)011
[58] Khachatryan V *et al* (CMS Collaboration) 2015 Measurement of J/ψ and ψ(2S) prompt double-differential cross sections in pp collisions at $\sqrt{s} = 7$ TeV *Phys. Rev. Lett.* **114** 191802
[59] Chatrchyan S *et al* (CMS Collaboration) 2012 Measurement of the relative prompt production rate of χ_{c2} and χ_{c1} in pp collisions at $\sqrt{s} = 7$ TeV *Eur. Phys. J.* C **72** 2251

[60] Aad G *et al* (ATLAS Collaboration) Measurement of the differential cross-sections of prompt and non-prompt production of J/ψ and ψ(2S) in pp collisions at $\sqrt{s} = 7$ and 8 TeV with the ATLAS detector arXiv:1512.03657
[61] Aad G *et al* (ATLAS Collaboration) 2014 Measurement of χ_{c1} and χ_{c2} production with $\sqrt{s} = 7$ TeV pp collisions at ATLAS *J. High Energy Phys.* JHEP07(2014)154
[62] Aaij R *et al* (LHCb Collaboration) 2012 Measurement of $\psi(2S)$ meson production in pp collisions at $\sqrt{s} = 7$ TeV *Eur. Phys. J.* C **72** 2100
[63] Aaij R *et al* (LHCb Collaboration) 2011 Measurement of J/ψ production in pp collisions at $\sqrt{s} = 7$ TeV *Eur. Phys. J.* C **71** 1645
[64] Aaij R *et al* (LHCb Collaboration) 2015 Measurement of forward J/ψ production cross-sections in pp collisions at $\sqrt{s} = 13$ TeV *J. High Energy Phys.* JHEP10(2015)172
[65] Aaij R *et al* (LHCb Collaboration) 2013 Measurement of the relative rate of prompt χ_{c0}, χ_{c1} and χ_{c2} production at $\sqrt{s} = 7$ TeV *J. High Energy Phys.* JHEP10(2013)115
[66] Baier R and Ruckl R 1983 Hadronic collisions: a quarkonium factory *Z. Phys.* C **19** 251
[67] Humpert B 1987 Narrow heavy resonance production by gluons *Phys. Lett.* B **184** 105
[68] Gastmans R, Troost W and Wu T T 1987 Production of heavy quarkonia from gluons *Nucl. Phys.* B **291** 731
[69] Cho P L and Leibovich A K 1996 Color octet quarkonia production *Phys. Rev.* D **53** 150
[70] Cho P L and Leibovich A K 1996 Color octet quarkonia production. 2 *Phys. Rev.* D **53** 6203
[71] Braaten E, Fleming S and Leibovich A K 2001 NRQCD analysis of bottomonium production at the Tevatron *Phys. Rev.* D **63** 094006
[72] Lai H L, Guzzi M, Huston J, Li Z, Nadolsky P M, Pumplin J and Yuan C-P 2010 New parton distributions for collider physics *Phys. Rev.* D **82** 074024
[73] Nakamura K *et al* (Particle Data Group Collaboration) 2010 Review of particle physics *J. Phys.* G **37** 075021
[74] Eichten E J and Quigg C 1994 Mesons with beauty and charm: spectroscopy *Phys. Rev.* D **49** 5845
[75] Zhang H F, Yu L, Zhang S X and Jia L 2016 Global analysis of the experimental data on χ_c meson hadroproduction *Phys. Rev.* D **93** 054033
Zhang H F, Yu L, Zhang S X and Jia L 2016 Global analysis of the experimental data on χ_c meson hadroproduction *Phys. Rev.* D **93** 079901